

High-Field High-Speed MAS Resolution Enhancement in ^1H NMR Spectroscopy of Solids

A. Samoson,* T. Tuherm,* and Z. Gan[†]

*National Institute of Chemical and Biophysics, Tallinn 12618, Estonia; and

[†]National High Magnetic Field Laboratory, Tallahassee, Florida 32310

Received April 27, 2001

Resolution in ^1H NMR spectra of solids can be significantly enhanced with fast magic-angle spinning and high magnetic fields. A variable field and spinning speed study up to 25 T and 40 kHz shows that the homogeneous line broadening is inversely proportional to the product of magnetic field strength and spinning speed. The combination of high field and fast speed yields a ^1H linewidth approaching the intrinsic limit determined by anisotropy of magnetic susceptibility. An analysis of the anisotropic magnetic susceptibility line broadening is presented. © 2001 Academic Press

Key Words: NMR; high field; MAS, dipolar interaction; line broadening, magnetic susceptibility.

I. INTRODUCTION

Line broadening mechanisms in solid-state NMR spectroscopy are classified as homogeneous and inhomogeneous [1]. The homogeneous line broadening is generated by randomly fluctuating local magnetic fields, whereas the inhomogeneous contribution comes from the local field that does not vary in the time scale of signal measurement and depends primarily on the spatial coordinates. Sample spinning at the magic-angle has been proven very efficient in removing the inhomogeneous part of broadening such as chemical shift anisotropy and magnetic field inhomogeneity [2–4].

The homogeneous part of the line broadening usually comes from dipolar interactions among abundant spins in solids that have high gyromagnetic ratios such as ^1H and ^{19}F . Mutual spin flip-flops that require little energy adjustment by lattice or external magnetic fields make the dipolar local field fluctuate at a time scale about the inverse of the mean dipolar coupling constant [5]. Magic-angle spinning is inefficient in averaging the randomly fluctuating local fields because the spinning speed is not fast compared to the ^1H homogeneous linewidth. Advances in sample spinning technology have started to change the situation and the speed dependence on MAS line narrowing has attracted a number of groups. Brunner *et al.* have derived the second moment based on the average Hamiltonian under fast MAS [6]. Their results show that the residual ^1H linewidth is proportional to the inverse of spinning speed and depends on the mutual orientation among dipolar coupling and chemical

shift anisotropy spin interaction tensors. A numerical study by Vega and colleagues indicates that the residual dipolar broadening is expected to follow mixed inverse power dependence on spinning speed in the range between -1 and -2 [7]. The spectral resolution also depends on the magnetic field strength. Higher magnetic fields increase the line separation between neighboring spins and may slow down the spin flip-flops, the main mechanism of local field fluctuations, leading to more efficient averaging by MAS.

In the past, multiple-pulse decoupling, first proposed by Waugh *et al.* [8], has remained the main technique for eliminating homonuclear dipolar interactions for high-resolution ^1H spectra of rigid solids. Improvement in pulse sequence performance and the combination of sample rotation have made the multiple-pulse approach capable of narrowing ^1H lines to intrinsic linewidth, mainly limited by the magnetic susceptibility of the samples [9–11]. Multiple-pulse decoupling requires strong B_1 fields, carefully tuned transmitters, and fast-recovered receivers [12, 13] and may become inefficient at high magnetic fields and fast spinning speed because of large frequency offsets and fast sample rotation which interferes with the coherence of spin motion. The experimental complications have prevented a widespread use of the technique even at modest fields and a more direct approach with fast MAS and high magnetic fields may be desirable.

We present an experimental study on field and speed dependence of MAS line narrowing over the entire range of both parameters, available according to the current level of technology. We have chosen rigid solid samples where homogeneous linewidth can reach 100 kHz and their ^1H resolution enhancement presents great practical interests. A model on the line broadening effect by anisotropic magnetic susceptibility is also presented as the explanation of inhomogeneous line broadening limits of the ^1H spectral resolution once most of the homogeneous part is suppressed.

II. EXPERIMENTAL

Single-pulse experiments were performed on a 1066-MHz resistive magnet and an 832-MHz superconductive magnet, both at the National High Magnetic Field Laboratory (NHMFL), and a 500-MHz magnet at the National Institute of Chemical Physics and Biophysics (NICBP). The resistive magnet adopted a split-coil design for a homogenous magnetic field [14] and the field homogeneity was further improved using ferromagnetic shim. The measurement with the resistive magnet was limited to single scan acquisition due to a temporal instability [15]. The overall effects from magnetic field inhomogeneity and instability contribute about 0.2-ppm additional linewidth. The MAS probe was built at the NICBP and it fits all three magnets including the 832-MHz superconductive magnet with 29-mm bore size. MAS spectra were acquired with spinning speed up to 40 kHz using MAS rotors of 2 mm in diameter, 10 mm in length, and 11 μL sample volume. The rotors were ground from metastablized zirconia and the rotation is supported by radial air bearing at both ends and driven by a tangential air jet to one of the polymer endcaps. The reduced rotor diameter enables the high spinning speed. The samples of glycine and deuterated malonic acid were used as directly obtained from Aldrich.

III. RESULTS AND DISCUSSION

Figure 1 shows a comparison of ^1H MAS spectra taken at 1066, 832, and 500 MHz with 40-kHz spinning speed. The fast spinning speed narrows the ^1H lines of the three nonequivalent sites in glycine.

Higher fields clearly improve the resolution through the field-dependent chemical shift. Remarkably, the results at the strongest superconductive and resistive magnets available at the time of measurements favor the resistive magnet in this case.

The quantitative measurements were performed on malonic acid. The methylene line of malonic acid is experimentally well separated from acidic protons and provides for direct linewidth measurement over a broad range of the field and speed values. Figure 2 plots the ^1H linewidth of the methylene peak in units of parts per million as a function of the inverse product of magnetic field strength and spinning speed $(B_0\nu_{\text{rot}})^{-1}$. The data from three magnetic field strengths and variable spinning speed indicate that the linewidth is nearly proportional to the inverse product of the two parameters. If measured in units of hertz, the linewidth would remain independent of field strength. This result suggests that the magnetic field fluctuations are mostly unchanged with the variation of field strength over the current experimental range. The inverse speed dependence ν_{rot}^{-1} of the ^1H linewidth agrees with the results from moment analysis [6], but is slightly different from the numerical simulations by Vega and colleagues. In numerical simulations, the dimension of Hilbert space grows exponentially with the number of spins in the system and the simulation of an infinite proton-coupled network in solids is impossible. Spin systems are usually truncated to a small and isolated group manageable for computer

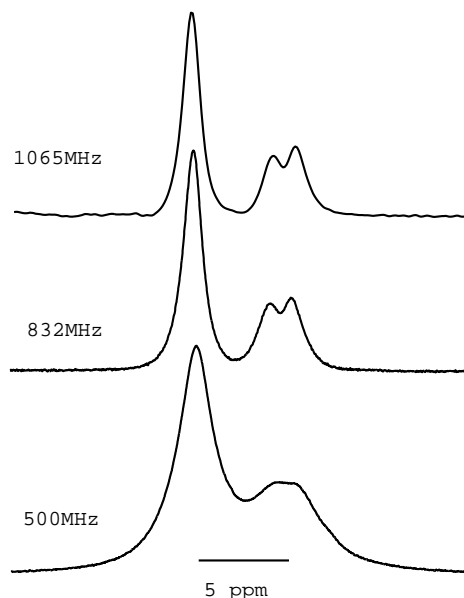


FIG. 1. ^1H spectra of glycine taken at 11.7, 19.6, and 25 T and 40-kHz MAS.

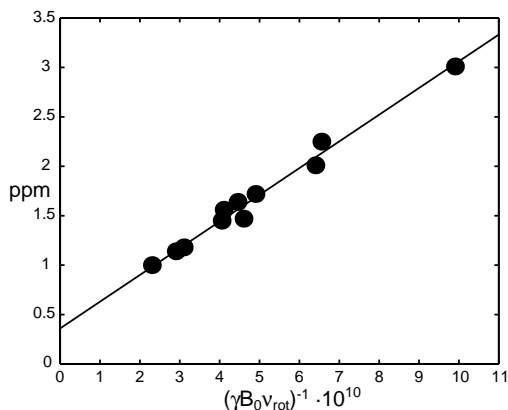


FIG. 2. ^1H linewidth vs $(\gamma B_0 \nu_{\text{rot}})^{-1}$. The full width at half-height of the methylene peak of malonic acid spectra was measured.

simulation. The effect of such a truncation is still unknown and the supplement of experimental data is helpful in finding suitable models for numerical simulations. A calculation in Liouville space may be able take account, in the form of relaxation, of the interaction of the isolated spin system to the rest of the protons.

In Fig. 2, an extrapolation of the data points to the infinite value of speed-field product predicts a homogeneous broadening free linewidth limit of 0.35 ppm. This can be compared with the data of a deuterated sample, where the residual protons are diluted and their local fields are mainly from the chemical shift anisotropy and heteronuclear dipolar coupling from neighboring deuterons (Fig. 3).

The spin flip-flops among deuterons are quenched by the large frequency offsets of quadrupolar couplings and weaker dipolar couplings. Since no speed dependency was observed at higher spinning rates, the measured 0.3 ppm can be assumed to

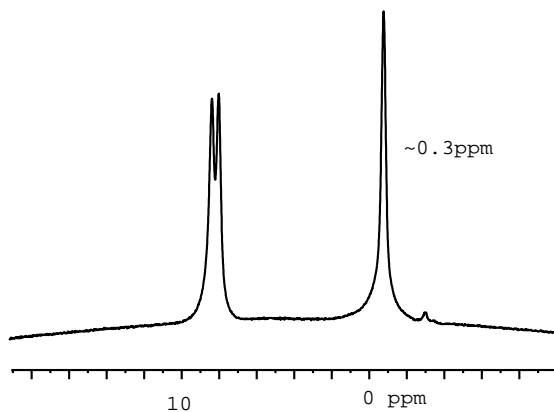


FIG. 3. ^1H spectrum of deuterated malonic acid with 40-kHz MAS.

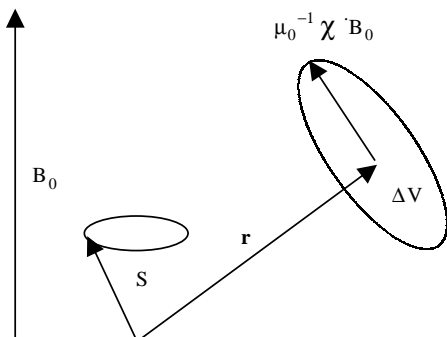


FIG. 4. Local field induced by anisotropic magnetic susceptibility.

represent inherent linewidth, free of homogeneous contribution. This linewidth is indeed in close agreement with the 0.35-ppm extrapolation in Fig. 2.

A major source of the remaining linewidth of polycrystalline samples comes from the anisotropic part of the magnetic susceptibility. Figure 4 illustrates the local field at spin S generated by an induced magnetic moment of the sample substance in volume ΔV . If the susceptibility is isotropic, the induced magnetic moment is constant and along the magnetic field and the local field to spin S is similar to a heteronuclear dipolar interaction that can be completely averaged by MAS. However, in general cases the anisotropic susceptibility tensor $\bar{\chi}$ introduces modulation of the induced magnetic dipolar moment \bar{M} ,

$$\bar{M} = \mu_0^{-1} \bar{\chi} \cdot \vec{B}_0 \Delta V. \quad (1)$$

The interaction between the induced magnetic moment and spin S can be rewritten in secular approximation as

$$H_\chi = \vec{S} \cdot \vec{D} \cdot \bar{M} = (D_{zx}\chi_{xz} + D_{zy}\chi_{yz} + D_{zz}\chi_{zz})\mu_0^{-1}S_zB_0\Delta V. \quad (2)$$

χ_{ij} are the Cartesian components of the susceptibility tensor and $D_{ij} = \frac{\mu_0\gamma}{4\pi r^3}(\delta_{ij} - 3\hat{r}_i\hat{r}_j)$ are similar to the components of dipolar interaction. The Hamiltonian can be written in irreducible spherical tensor components $D_{2,m}$ and $\chi_{2,m}$ with $D_{zx} = \frac{D_{2,-1} - D_{2,1}}{2}$,

$$D_{zy} = \frac{D_{2,-1} + D_{2,1}}{2i}, \quad D_{zz} = \sqrt{\frac{2}{3}}D_{2,0} \quad (3)$$

$$H_\chi = \left[-\frac{1}{2}(D_{2,1}\chi_{2,-1} + D_{2,-1}\chi_{2,1}) + \frac{2}{3}D_{2,0}\chi_{2,0} \right] \mu_0^{-1}S_zB_0\Delta V.$$

The product of two second-rank tensor components can be expanded using the Clebsch–Gordon series

$$\begin{aligned}
 H_\chi &= \left[\sqrt{\frac{1}{5}}W_{0,0} - \sqrt{\frac{1}{14}}W_{2,0} - \sqrt{\frac{8}{35}}W_{4,0} + \frac{2}{3} \left(\sqrt{\frac{1}{5}}W_{0,0} - \sqrt{\frac{2}{7}}W_{2,0} + \sqrt{\frac{18}{35}}W_{4,0} \right) \right] \\
 &\quad \times \mu_0 S_z B_0 \Delta V \\
 &= \left(\sqrt{\frac{5}{9}}W_{0,0} - \sqrt{\frac{7}{18}}W_{2,0} \right) \mu_0^{-1} S_z B_0 \Delta V,
 \end{aligned} \tag{4}$$

using

$$W_{l,0} = \sum_m c(22l, m - m) D_{2,m} \chi_{2,-m}. \tag{5}$$

It is interesting to note that here the $W_{4,0}$ term vanishes, quite contrary, e.g., to the second-order quadrupolar effect where the product of two second-rank components contributes to the $W_{4,0}$ term. The absence of the $W_{4,0}$ term is indirectly corroborated also by comparison of the residual linewidth from MAS and DOR measurements on spin $S = 1/2$ nuclei under high magnetic fields.

Magic-angle spinning averages out the $W_{2,0}$ term and the local field from the anisotropic magnetic susceptibility causes a shift of peak position,

$$\Delta\omega_\chi = \frac{1}{3} (D_{2,2}\chi_{2,-2} - D_{2,1}\chi_{2,-1} + D_{2,0}\chi_{2,0}) \mu_0^{-1} B_0 \Delta V. \tag{6}$$

The isotropic shift is independent of the reference frame and in a frame with z -axis along the distance vector

$$\Delta\omega_\chi = \frac{2}{9} D_{zz} \chi_{zz} \mu_0^{-1} B_0 \Delta V = -\frac{\omega_L}{9\pi} \frac{\chi_D}{r_3} \Delta V, \tag{7}$$

where χ_D is the susceptibility tensor component along the distance vector \hat{r} (Fig. 1) and ω_L is the Larmor frequency. An integration of the contribution from the whole sample gives the net shift from the anisotropic magnetic susceptibility effect.

$$\omega_\chi = -\frac{\omega_L}{9\pi} \int \frac{\chi_D}{r_3} dV \tag{8}$$

Considering a large single crystal with negligible boundary effect, the integration over unit sphere $\int \chi_D d\Omega$ vanishes. However, for polycrystalline samples, statistical differences in local packing order around any given spin are expected. The local variations sum up to a spread of resonance lines for the sample as a whole generated by the shift in Eq. (8). This line broadening effect is proportional to the Larmor frequency and remains constant if measured in parts per million. This mechanism of the residual susceptibility broadening was demonstrated in the elegant experimental work by Alla and Lippmaa [16].

IV. CONCLUSIONS

The experimental study has demonstrated new possibilities of ^1H resolution enhancement in solids with high-speed MAS and high magnetic fields. At the current technological level the homogeneous linewidth is still larger than the susceptibility determined “natural” linewidth. In the studied sample, these values may become equal if the product of the field and sample spinning is increased by a factor of 2.

ACKNOWLEDGMENTS

This work is supported by the Estonian Science Foundation and by the National Science Foundation through the cooperative agreement DMR-9527035 with the National High Magnetic Field Laboratory.

REFERENCES

1. M. Maricq and J. S. Waugh, *J. Chem. Phys.* **70**, 3300 (1979).
2. E. R. Andrew, A. Bradbury, and R. G. Eades, *Nature* **182**, 1659 (1958).
3. I. J. Lowe, *Phys. Rev. Lett.* **2**, 285 (1959).
4. J. Schaefer and E. O. Stejskal, *J. Am. Chem. Soc.* **98**, 1031 (1976).
5. A. Abragam, “Principles of Nuclear Magnetism,” Oxford Univ. Press, Oxford (1961).
6. E. Brunner, D. Freude, B. Gerstein, and H. Pfeifer, *J. Magn. Reson.* **90**, 90 (1990).
7. S. Ray, E. Vinogradov, G.-J. Boender, and S. Vega, *J. Magn. Reson.* **135**, 418 (1998).
8. J. S. Waugh, L. M. Huber, and U. Haeberlen, *Phys. Rev. Lett.* **20**, 180 (1968).
9. W. K. Rhim, D. D. Elleman, and R. W. Vaughan, *J. Chem. Phys.* **59**, 3740 (1973).
10. D. Burum and W.-K. Rhim, *J. Chem. Phys.* **71**, 944 (1979).
11. R. E. Taylor, P. G. Pembleton, L. M. Ryan, and B. C. Gerstein, *J. Chem. Phys.* **71**, 4541 (1979).
12. D. P. Burum, M. Linder, and R. R. Ernst, *J. Magn. Reson.* **43**, 463 (1981).
13. B. C. Gerstein and C. R. Dybowski, “Transient Techniques in NMR of Solids,” Academic Press, New York (1985).
14. Y. M. Eyssa, M. Bird, B. J. Gao, and H. J. Schneider-Muntau, *IEEE Trans. Magn.* **32**, 2452 (1996).
15. V. Soghomonian, M. Cotton, R. Rosnske, and T. Cross, *J. Magn. Reson.* **125**, 212 (1997).
16. M. Alla and E. Lippmaa, *Chem. Phys. Lett.* **87**, 30 (1982).